ELECTRONIC SUPPORTING INFORMATION

High-Rate Synthesis of Cu-BTC Metal-Organic Frameworks

Ki-Joong Kim,[a,b] Yong Jun Li,[a,b] Peter B. Kreider,[a] Chih-Hung Chang,*[a,b] Nick Wannenmacher,[a] Praveen K. Thallapally,[c] and Ho-Geun Ahn[d] *Correspondence and requests for materials should be addressed to C-H.C. (chih-hung.chang@oregonstate.edu)

[a] School of Chemical, Biological & Environmental Engineering, Oregon State University, Corvallis, Oregon 97331, United States

[b] Oregon Process Innovation Center, Microproducts Breakthrough Institute, Corvallis, Oregon 97330, United States

[c] Pacific Northwest National Laboratory, Richland, Washington 99352, United States

[d] Department of Chemical Engineering, Suncheon National University, Sunchon, Jeonnam 540-742, South Korea

Experimental details

Sample preparation

The Cu-BTC metal-organic frameworks were synthesized by a continuous-flow microreactor-assisted (CFMA) system (shown in Fig. S1), which consisted of feeding, mixing, reaction, and cooling zones. Copper(II) nitrate hexahydrate ($Cu(NO_3)_2 \cdot 6H_2O$, 3.6 mmol, Alfa Aesar) solution in water or ethanol (60 mL) and benzene-1,3,5-tricarboxylic acid (BTC, 8.1 mmol, Aldrich) solution in ethanol (60 mL) were each separately stirred for 10 min in a 250 mL beaker. The $Cu(NO_3)_2 \cdot 6H_2O$ and BTC precursors were pumped through a stainless steel micro T-mixer (0.75 mm bore, Valco) with HPLC pumps (P-2010, Chrom Tech Series III) at a flow rate of 1 mL min^{-1}. The mixture entered into a stainless steel tubing reaction zone (30 cm long and 1.59 mm I.D.), where the reaction temperatures (60, 120, and 160 °C) were controlled by a temperature controller (SD PID temperature controller, Watlow). The reaction solution was then quenched in a water jacket heat exchanger (20 cm long and 1.59 mm I.D.). A back-pressure regulator (Swagelok) was installed after the cooler to maintain a constant pressure (100 bar) to ensure the mixture remained liquid at reaction temperatures. The resulting products were collected in a glass vial. The different reaction conditions used in the synthesis of Cu-BTC are summarized in Table S1.

For comparison, Cu-BTC synthesized via a typical solvothermal method in the batch reactor was also prepared. A solution of $Cu(NO_3)_2 \cdot 6H_2O$ (3.6 mmol) in 60 mL of solvent consisting of equal parts ethanol and water, and BTC (8.1 mmol) in 60 mL of ethanol were both stirred for 10 min in a 250 mL beaker, separately. A 50/50 mixture of $Cu(NO_3)_2$ and BTC solution was stirred for

10 min, then placed into a Teflon autoclave. The sealed autoclave was heated to 120 °C, held for 18 h in a convective oven, and then cooled to room temperature naturally.

The collected reaction products of both methods were centrifuged at 6000 rpm for 10 min. The supernatant was discarded and 10 mL of ethanol was added, followed by sonication for 5 min. The above centrifugation and sonication procedures were repeated 3 times to further purify Cu-BTC product. The final product was dried under vacuum for 24 h at 70 °C and held for further characterization.

Characterization

Powder X-ray diffraction patterns were obtained using a Bruker D8 Discover, operating at 40 kV and 40 mA with Cu kα_1 radiation (0.154 nm) in the 2θ scan range from 5° to 30° with a step size of 0.05°. Raman spectra were recorded using a WITec confocal Raman microscope with an Ar ion laser (514 nm) and a CCD detector. Nitrogen adsorption/desorption isotherms were measured at -196 °C with a Micromeritics ASAP 2010 analyzer. The samples were degassed in vacuum for 2 h at 150 °C prior to analysis. The Brunauer-Emmett-Teller surface areas (S_{BET}) were obtained from the amount of N_2 physisorbed at different relative pressures (P/P_0), based on the linear part of the 6 point adsorption data at P/P_0 = 0.02 - 0.10. The total pore volume (V_{total}) was calculated by the Horvath Kawazoe method at P/P_0 = 0.99. The mesopore volume (V_{meso}) and micropore volume (V_{micro}) were obtained by the Barrett-Joyner-Halenda adsorption and the *t*-plot methods, respectively. The pore size distribution was evaluated by the original density functional theory model. Field emission-scanning electron microscope (FE-SEM) analysis was conducted with an FEI Quanta 600 using 5-10 kV accelerating voltage. A thin gold/palladium layer was coated on the samples to increase its electrical conductivity. Thermal gravimetric analysis was performed on a TA instrument, SDT Q600. The sample (~ 10 mg) was placed into an alumina crucible and heated under N_2 flow (100 mL min^{-1}) at a rate of 20 °C min^{-1} up to 450 °C.

References

S1. M. Klimakow, P. Klobes, A. F. Thunemann, K. Rademann and F. Emmerling, *Chem. Mater.*, 2010, **22**, 5216-5221.

S2. J. Hafizovic, M. Bjorgen, U. Olsbye, P. D. C. Dietzel, S. Bordiga, C. Prestipino, C. Lamberti and K. P. Lillerud, *J. Am. Chem. Soc.*, 2007, **129**, 3612-3620.

S3. E. Biemmi, A. Darga, N. Stock and T. Bein, *Microporo. Mesoporo. Mater.*, 2008, **114**, 380-386.

S4. Z. Qin, B. Shen, X. Gao, F. Lin, B. Wang and C. Xu, *J. Catal.*, 2011, **278**, 266-275.

S5. S. Morin, P. Ayrault, N. S. Gnep and M. Guisnet, *Appl. Catal. A: Gen.,* 1998, **166**, 281-292.

S6. A. H. Janssen, A. J. Koster and K. P. de Jong, *J. Phys. Chem. B.,* 2002, **106**, 11905-11909.

S7. A. Vishnyakov, P. I. Ravikovitch, A. V. Neimark, M. Bu1low and Q. M. Wang, *Nano Lett.,* 2003, **3**, 713-718.

S8. V. Krungleviciute, K. Lask, L. Heroux, A. D. Migone, J.-Y. Lee, J. Li and A. Skoulidas, *Langmuir,* 2007, **23**, 3106-3109.

Tables

Table S1. Different reaction conditions used in the batch and CFMA methods

Samples	Solvents		Temperature
	$Cu(NO_3)_2$ (mL)	BTC (mL)	(°C)
Brxn	Water (30)/ethanol (30)	Ethanol (60)	120
Crxn1	Water (30)/ethanol (30)	Ethanol (60)	120
Crxn2	Water (60)	Ethanol (60)	120
Crxn3	Ethanol (60)	Ethanol (60)	120
Crxn4	Ethanol (60)	Ethanol (60)	60
Crxn5	Ethanol (60)	Ethanol (60)	160

* Brxn and Crxn denote the samples synthesized by batch and CFMA methods, respectively.

Table S2. Physisorption properties of the samples synthesized by batch and CFMA methods

Samples	S_{BET}	Pore volumes ($cm^3\ g^{-1}$)		
	($m^2\ g^{-1}$)[a]	V_{total}[b]	V_{meso}[c]	V_{micro}[d]
Brxn	886	0.441	0.078	0.364
Crxn1	848	0.562	0.214	0.324
Crxn2	439	0.229	0.048	0.211
Crxn3	995	0.594	0.137	0.406
Crxn4	1673	0.714	0.103	0.636
Crxn5	773	0.432	0.158	0.263

[a] BET surface area. [b] Total pore volume. [c] Mesopore volume. [d] Micropore volume. S_{BET} shows 886 $m^2\ g^{-1}$ for Brxn and 848 $m^2\ g^{-1}$ for Crxn1. V_{total} and V_{micro} of Crxn1 are estimated to be 0.562 $cm^3\ g^{-1}$ and 0.324 $cm^3\ g^{-1}$, respectively. S_{BET} of Brxn is a slightly higher than Crxn1, but V_{total} shows an opposite result. This is due to the higher proportion of V_{meso} in the Crxn1, with about 38 % of V_{total} attributable to mesopores, compared to about 18% in the Brxn. Crxn2 synthesized using pure water in $Cu(NO_3)_2$ solution shows a significantly lower S_{BET} of 439 $m^2\ g^{-1}$ and V_{total} of 0.229 $cm^3\ g^{-1}$. Crxn3, synthesized at 120 °C using pure ethanol in $Cu(NO_3)_2$ solution, showed even higher S_{BET} of 995 $m^2\ g^{-1}$ and V_{total} of 0.594 $cm^3\ g^{-1}$ than Crxn1 and Crxn2 samples.

Figures

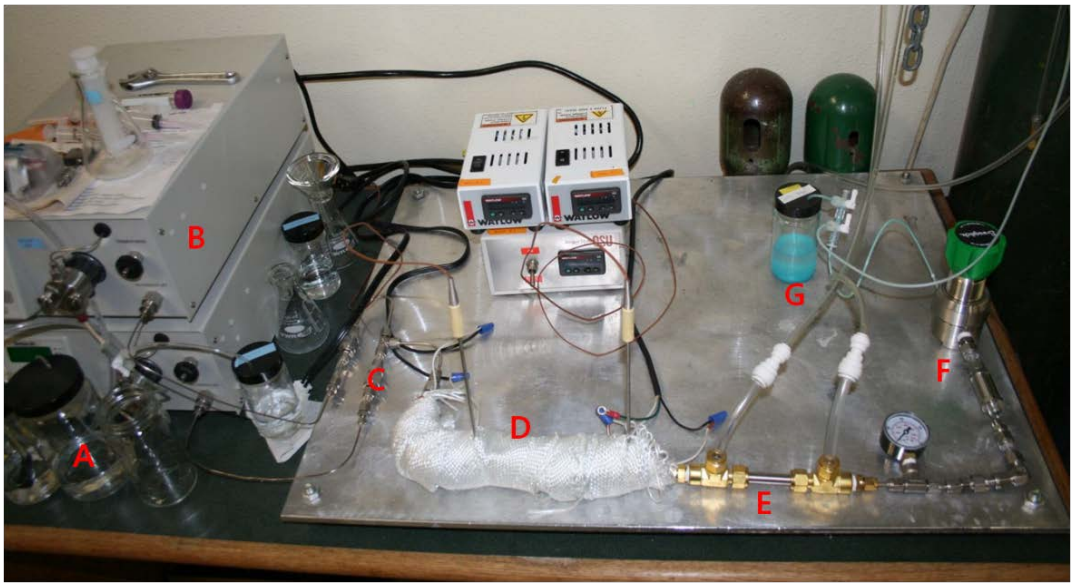

Fig. S1. Photograph of the CFMA system used for the high-rate synthesis of Cu-BTC. (A) Precursors in solutions, (B) HPLC pumps, (C) Mixing zone, (D) Reaction zone, (E) Cooling zone, (F) Back-pressure regulator, and (G) Collecting zone.

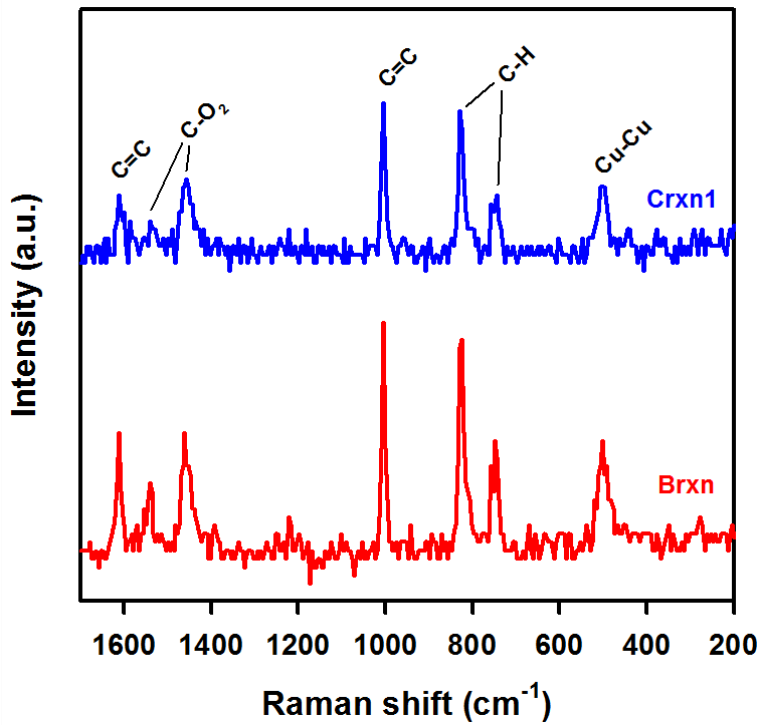

Fig. S2. Raman spectra of the Brxn and Crxn1 samples. Raman spectra were dominated by the organic bonding of the MOF framework, such as C-C, C=C, and C-H. Raman bands were found at 1611 and 1004 cm^{-1}, which correspond to the υ(C=C) modes of the benzene ring; the bands at 824 and 742 cm^{-1} correspond to out-of-plane ring (C-H) bending vibrations and to out-of-plane ring bending. The bands at 1540 and 1460 cm^{-1} are due to the $\upsilon_{asym}(C\text{-}O_2)$ and $\upsilon_{sym}(C\text{-}O_2)$ stretching modes. The band at 500 cm^{-1} is associated (Cu-Cu) modes in the low-frequency region (600-170 cm^{-1} range).[S1]

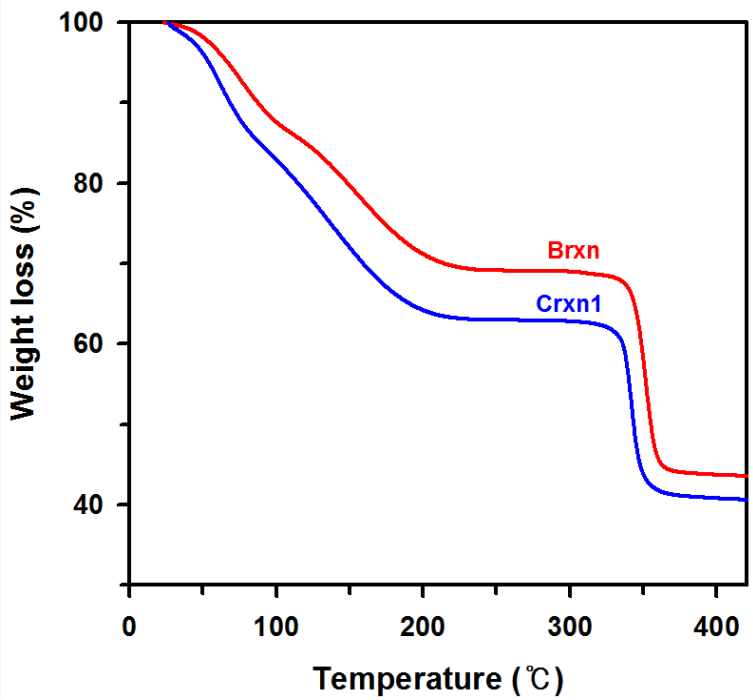

Fig. S3. TGA results of the Brxn and Crxn1 samples. Both samples show three distinct regions, indicating three different kinds of weight loss in the samples. The first weight loss region between room temperature and 85 °C can be assigned to the removal of the surface water molecules.[S2] The next weight loss of about 20% is observed in the range 85-200 °C which is due to the removal of the water molecules present in the channels and coordinated to the metal centers of the structure. The dehydrated samples are thermally stable up to 330 °C. In the next step, above 330 °C, a weight loss of 18% for Brxn and 22% for Crxn1, respectively, are observed and correspond to the decomposition of the tricarboxylate linker.[S3]

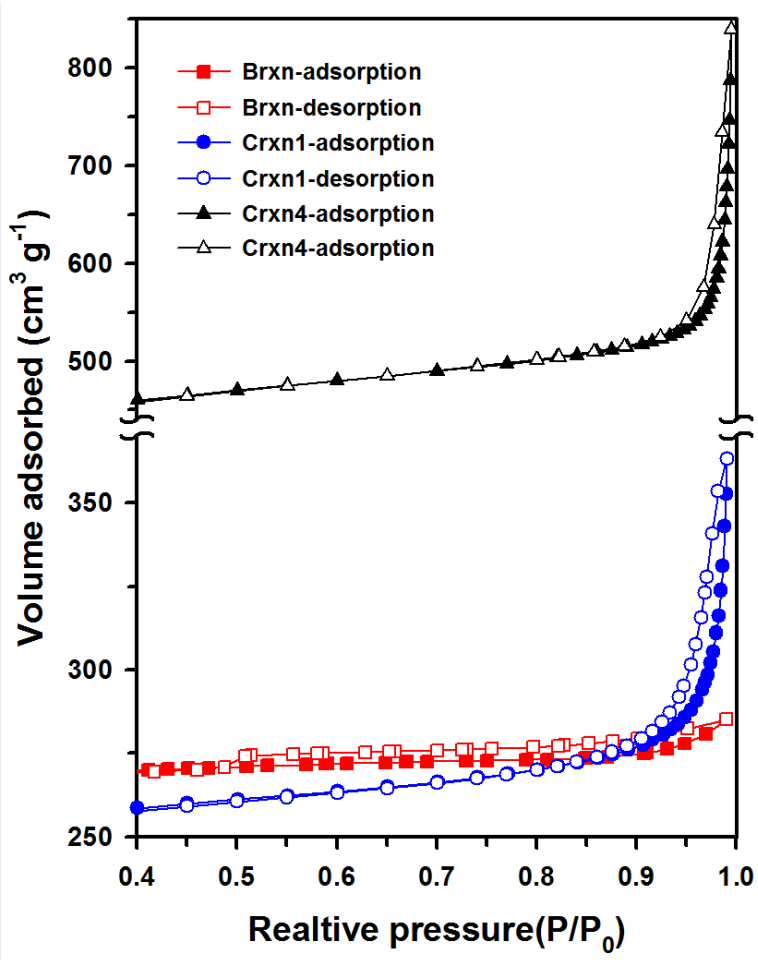

Fig. S4. Comparison of N_2 isotherms from the Brxn, Crxn1 and Crxn4 samples in the range of P/P_0 = 0.4 - 1.0. According to the IUPAC classification, Type I isotherms are characteristic of microporous materials rapidly increased at a lower P/P_0, while Type IV isotherms typically have a hysteresis loop associated with capillary condensation in the mesoporous structures. Brxn shows a Type I isotherm and a very small and wide hysteresis loop at P/P_0 = 0.5 to 0.9, which is typical for mesoporous structures with ink-bottle types pores smaller than 4 nm.[S4] A vertical hysteresis loop of Crxn samples in the narrow range of P/P0 = 0.9 to 1.0 indicates the presence of cylindrical type mesopores.[S5,S6]

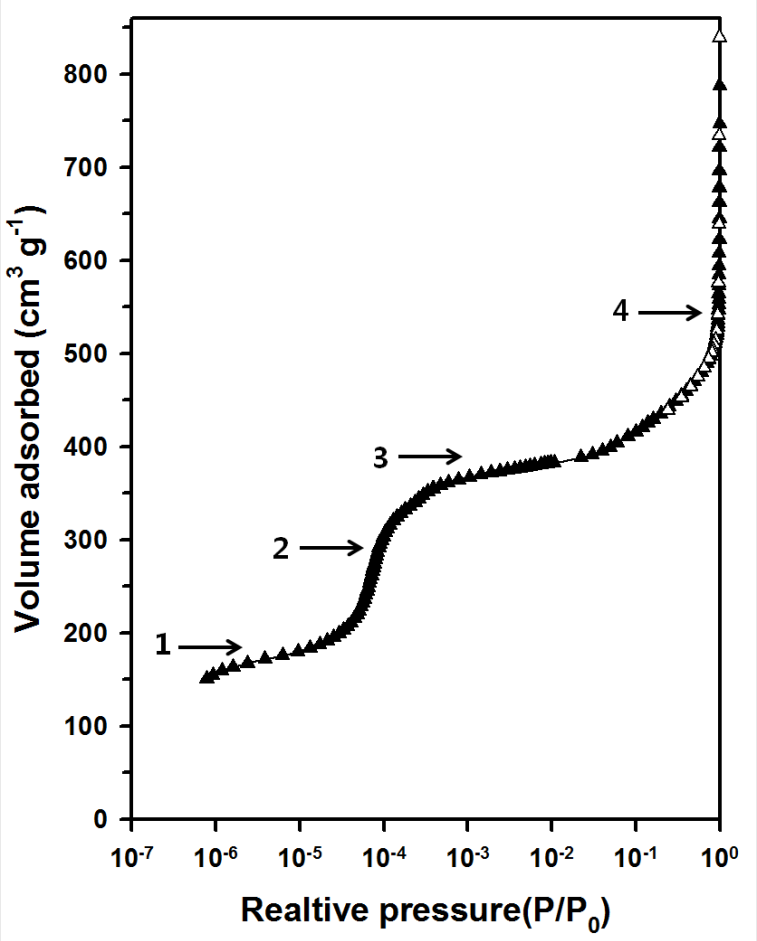

Fig. S5. Logarithmic N_2 gas isotherm of the Crxn4 sample. High-resolution measurements at extremely low pressures allowed linear interval of the adsorption isotherm at $P/P_0 < 10^{-6}$ where the adsorbate-adsorbate interactions can be neglected. The isotherm on a logarithmic relative pressure shows four different sub-regions. The first region (1) is attributed to adsorption in the tetrahedral side pockets (~ 0.35 nm diameter channels), the second region (2) to adsorption in the main channels (~ 0.9 nm diameter channels), the third (3) to the adsorbed molecules inside any voids formed when Cu-BTC crystals agglomerated into larger particles, and fourth region (4) to the some large macropores, most probably from intra-agglomerate voids in the sample.[S7,S8]